Research Article

Assessment of Spectral Wave Model Performance Using Three Wind Speeds in the Eastern Mediterranean Sea

Fulya Islek[*] iD , Yalcin Yuksel iD , Furkan Yuksel iD

Civil Engineering, Faculty of Civil Engineering, Yildiz Technical University, Istanbul, TURKIYE

Abstract

The main aim of the present study is to evaluate and validate the performance of the MIKE 21 SW (Spectral Wave) model using the three different wind fields in the Eastern Mediterranean Sea. To achieve the goal, the wind data were downloaded from the European Centre for Medium-Range Weather Forecasts (ECMWF) ERA-Interim, ECMWF ERA5, and the National Centers for Environmental Prediction (NCEP) Climate Forecast System Reanalysis (CFSR) datasets. Model results were calibrated with four buoy measurements (Alanya, Bozcaada, Dalaman, and Antalya stations) by tuning physical model parameters. As a result of calibration studies, it was determined that the wave simulations showed a strong sensitivity to the whitecapping parameter (C_{ds}) compared to other physical parameters. Calibrated MIKE 21 SW model run to validate at two buoy measurements (Dardanelles and Silifke stations). Considering the results of statistical investigations: (i) ERA-Interim predicted lower significant wave heights and wave periods than those obtained with ERA5 and CFSR, i.e., underestimated, (ii) CFSR slightly overestimated the wave data compared to results for ERA5 and ERA-Interim, (iii) ERA5 performed slightly better than ERA-Interim in hindcasting of Eastern Mediterranean wave properties. It can be said that the wave characteristics obtained with ERA5 exhibited a slightly better fit with the Eastern Mediterranean wave measurements compared to those obtained with the other two datasets (ERA-Interim and CFSR).

Keywords: MIKE 21 SW, Mediterranean Sea, ERA-Interim, ERA5, CFSR, wave model calibration

Introduction

Long-term reliable information on wave climate and extreme wave statistics requires sufficiently large datasets (Swain, 1997). Owing to some challenges such as the lack of continuous long-wave measurements, having only significant wave height records in altimeter data, satellite data missing extreme events, and providing information with a high spatial resolution and long duration, the wave hindcast is one of the best alternative methods to obtain long-term wave datasets. Since the last quarter of the 20th century, spectral wave models such as WAM (WAMDI, 1988), Wavewatch (Tolman, 1991), SWAN (Simulating WAves Nearshore) (Booij et al., 1999), and MIKE 21 SW (Spectral Wave) (DHI, 2007), which use high-quality wind fields as input data, have been widely used.

Numerous studies on the spectral wave models have been implemented in the Mediterranean Sea; Cavaleri and Bertotti (2005) simulated several periods using different resolutions of the ECMWF (European Centre for Medium-Range Weather Forecast) meteorological model and assessed the quality of the surface wind and wave model results varies with the resolution. The authors noted that in enclosed seas such as the Mediterranean Sea, the errors decrease with increasing resolution, but a substantial underestimate remains. Another implementation of the WAM model was used by Music and Nikovic (2008) to evaluate the prediction

of Eastern Mediterranean Sea wave fields for a 44-year period (1958−2001). The WAM model was driven by wind data generated from the regional atmospheric model REMO. Ponce de Leon and Soares (2008) compared the wave hindcast in the Western Mediterranean Sea using the reanalysis wind fields from HIPOCAS (Hindcast of Dynamic Processes of the Ocean and Coastal Areas of Europe) and ERA-40 from ECMWF for November 2001. Mentaschi et al. (2015) analyzed the performance of the wave model Wavewatch III in the Mediterranean Sea. The wind employed in the simulations was provided by Weather Research and Forecast (WRF-ARW) version 3.3.1 for a 32-year period (1979−2010). Yuksel et al. (2020) investigated the effect of long-term variation of wave parameters and the Eastern Mediterranean Sea was modeled by the MIKE 21 SW model using 40-year (1979−2018) ERA-Interim wind fields. Vannucchi et al. (2021) focused on the wind-wave climate in the North-Western Mediterranean Sea and used a 29-year wind/wave hindcast (1990−2018) by downscaling the ERA5 global atmospheric reanalyzes. Elkut et al. (2021) evaluated the SWAN model performance using 31-year (1988−2018) ERA-Interim data along the Mediterranean Sea.

These previous studies agree that using high-quality wind fields as input data improves the accuracy of wave models. Significant improvements and innovative

features have been made in the reanalysis quality, recently, including developments in model physics and core dynamics, advanced data assimilation techniques, detailed records of global records of the global atmosphere, land surface, and ocean waves, and higher spatial and temporal resolution. For these reasons, the ECMWF's recent new reanalysis, ERA5 reanalysis of the global weather and climate, is of outstanding interest. However, there is a limited number of studies on the quality of ERA5 reanalysis wind data, and its contribution to wave model performance is fully unknown.

The present study aims to fill this gap by performing comparative analyses that determine the effect of different qualities of wind-forcing fields on wave model performance. For this purpose, the three different wind sources (ERA-Interim, ERA5, CFSR) were utilized to assess the performance of the MIKE 21 SW model in the hindcast of wave properties in the Eastern Mediterranean Sea. Model results were calibrated with four buoy measurements and validated with two buoy measurements from different locations along the Eastern Mediterranean Sea. Model performance forced by the wind fields with different spatial and temporal resolutions was evaluated using statistical error measures.

Materials and Methods
Study area

The study area covering approximately 893285 km^2 includes the Eastern Mediterranean Sea from 22°E to 36.5°E longitudes and 30.5°N to 41.5°N latitudes (Figure 1). The Aegean Sea is connected to the Sea of Marmara by the Dardanelles Strait and is connected to the Atlantic Ocean via the Strait of Gibraltar. The semi-closed basin shows different wave climate characteristics due to complex orography and coastlines (Elkut et al., 2021). The region has attracted the attention of many researchers.

Fig. 1. Study area and locations of the wave measurement stations.

Materials
In this study, the three different wind sources (ERA-Interim, ERA5, CFSR) were used to evaluate spectral wave model performance in the Eastern Mediterranean Sea. All wind fields were downloaded from the horizontal wind components at 10 m above the sea surface.

ERA-Interim (hereafter ERA-I) reanalysis dataset (Dee et al., 2011) is a well-known global wind source with a 6-h temporal resolution and can be obtained from ECMWF. ERA-I project was terminated on 31 August 2019 and data is available from 1 January 1979 to 31 August 2019. Originally, the ERA-I reanalysis dataset is available as a gridded dataset at the approximate spatial resolution of 0.7°x0.7° from the native T255 spectral grid. The spatial and temporal resolutions used in this study are 0.25°x0.25° and 6-h, respectively.

ERA5 (Hersbach et al., 2016) is the most recent reanalysis dataset produced by the ECMWF. This reanalysis replaced the highly successful ERA-I reanalysis and spans from 1950 to the present. ERA5 has many improvements relative to ERA-I including its higher spatial (0.3°x0.3°) and temporal (hourly) resolution. In the study, the wind speed components at 10-m height with a 0.25°x0.25° spatial resolution and hourly temporal resolution were obtained from ECMWF.

NCEP (National Centers for Environmental Prediction) CFSR (Climate Forecast System Reanalysis) (Saha et al., 2010), and CFSv2 (Saha et al., 2014) use the same model, but CFSv2 was an improved version. CFSR reanalysis data covers the period in version 1 from 1979

to 2010 and version 2 from 2011 to the present. The available resolutions for CFSR reanalysis datasets are between 0.312°×0.312° to 2.5°×2.5° for version 1, between 0.312°×0.312° and 2.5°×2.5° for version 2. Hourly temporal resolution exists in both versions. For the sake of consistency, CFSR (v1 and v2) reanalysis wind fields were downloaded with a spatial resolution of 0.5°×0.5° which is the finest resolution for both datasets.

In this study, ERA-I and ERA5 were downloaded with an upscaled spatial resolution of 0.25°x0.25° in both longitude and latitude and temporal resolutions of 6-h and 1-h, respectively. For CFSR wind fields, the temporal and spatial resolutions are selected as 1-h and 0.5°×0.5°, respectively.

Methods
MIKE 21 SW (Spectral Wave), the third-generation spectral wave model, was implemented to generate wave data in the Eastern Mediterranean Sea. The model can calculate the main physical mechanism of generation, transformation, and dissipation of wind waves and swells. The governing equation is based on the fully spectral formulation with the wave action conservation equation (Holthuijsen et al., 1989). The model is based on flexible and unstructured meshes which allow simultaneous computation at coarser regional scales and finer local scales. Further information about the MIKE 21 SW model can be found in the DHI (2007).

In the modeling area, unstructured spatial discretization was used to implement finer mesh in the coastal and shallow water areas. For more precise results and computational speed, different mesh resolution generated from the Mesh Generator module of MIKE Zero (DHI, 2007) was tested. The optimized computational mesh consists of 4098 nodes and 7035 triangular elements given in Figure 2. In this study, the bathymetric data of the Eastern Mediterranean Sea were obtained from the Turkish Naval Forces Office of Navigation, Hydrology, and Oceanography (ONHO) and were interpolated onto the model domain. The bathymetric data and computational mesh considered in the study for the Eastern Mediterranean Sea are presented in Figure 2. To evaluate the model performance on different wind sources, the three different wind fields (ERA-Interim, ERA5, and CFSR) were considered in the Eastern Mediterranean wave simulations.
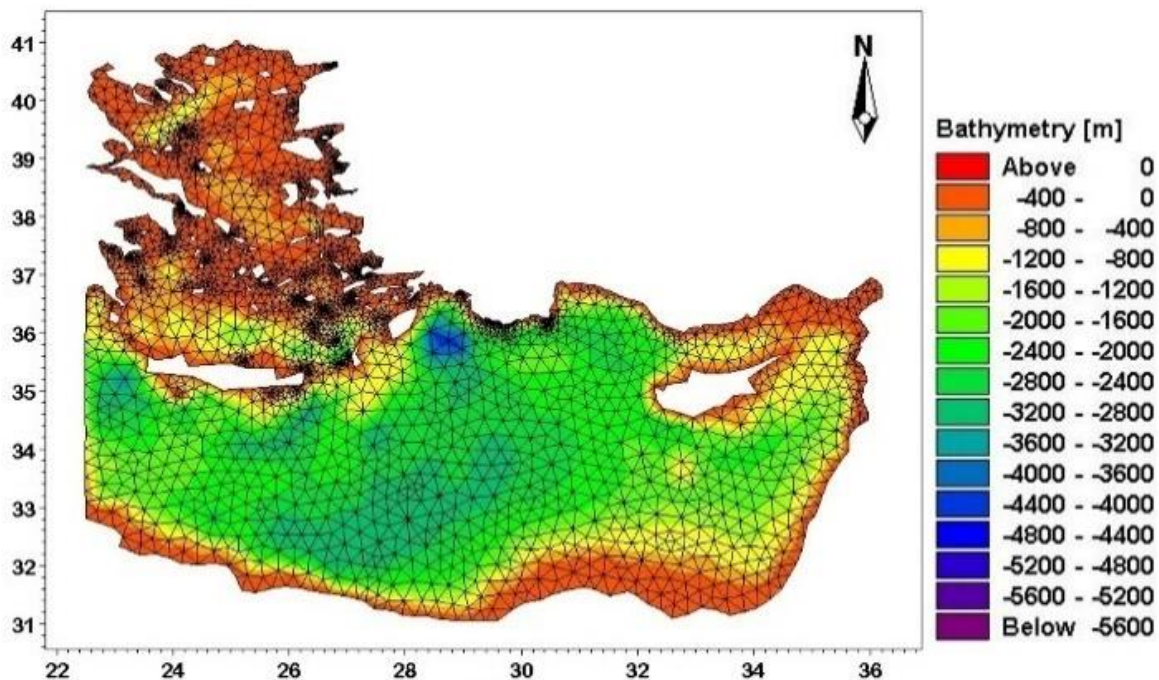

Fig. 2. Bathymetric map and computational mesh for the Eastern Mediterranean Sea.

In the simulations, the model reproduces the main physical processes such as generation and growth of wind waves, triad and quadruplet wave interactions, dissipation of wave energy due to whitecapping, bottom friction, and depth-limited wave breaking, refraction, diffraction, and shoaling of the waves during the propagation (DHI, 2007). The initial condition of each run of MIKE 21 SW is a JONSWAP fetch growth expression, which is the default (DHI, 2007). The lateral boundary condition was defined at the open boundary. Wave characteristics were generated from the MIKE 21 SW for a 25-year timespan (1994−2018) for which measurement wave data are available.

The performance of the implemented wave model was evaluated by calibration of several parameters related to physical processes. In the evaluation of the model performance, several statistical error measures were used, such as the bias, defined as the mean of differences between predicted and measured values, root means square error (RMSE); scatter index (SI), which represents the RMSE normalized to the mean observed values, and correlation coefficient (R). Bias, RMSE, SI, and R are calculated as follows:

$$Bias = \frac{1}{N}\sum_{i=1}^{N}(\bar{P} - \bar{O}) \qquad (1)$$

$$RMSE = \sqrt{\frac{1}{N}\sum_{i=1}^{N}(P_i - O_i)^2} \qquad (2)$$

$$SI = \frac{RMSE}{\bar{O}} \qquad (3)$$

$$R = \frac{\sum_{i=1}^{N}((P_i-\bar{P})(O_i-\bar{O}))}{\sqrt{\sum_{i=1}^{N}(P_i-\bar{P})^2(O_i-\bar{O})^2}} \qquad (4)$$

where N is the number of data, P_i is the hindcast value, O_i is the measured value, and the overbar shows the averages of the measurements and hindcasts.

The model was run for different calibration scenarios by changing the model meshes with different resolutions and different spectral and directional discretization, by adjusting the physical model parameters. Their effects on wave results (e.g., significant wave height, mean wave period, and peak wave period) were investigated and the final values were determined as follows:

➤ the formulation of Komen et al. (1994) for the parameterization of the wind input source term.
➤ Quadruplet-wave interaction was calculated by using the Discrete Interaction Approximation (DIA) proposed by Hasselmann et al. (1985).
➤ Triad wave interactions were opted out.
➤ Dissipation due to whitecapping was considered the formulation of Komen et al. (1994) and includes two dissipation coefficients. The selected values for C_{ds} and δ were 1.0−3.0 and 0.8, respectively.
➤ Constant Nikuradse roughness k_n with the value of 0.04 m was selected for dissipation due to bottom friction.
➤ The bore model proposed by Battjes and Janssen (1978) with $\alpha=1$ and $\gamma=0.8$ was used for dissipation due to the depth-limited wave breaking.
➤ The frequency discretization was defined between 0.04 Hz and 1.0 Hz on a logarithmic scale.

➤ The directional discretization was selected as 16 directional bins.
➤ The model was run with a calculation time step of 10 min and an output time step of 1 h.

Model simulations performed for different calibration scenarios did not show sensitivity to the parameters such as bottom friction, depth-induced wave breaking, and nonlinear wave-wave interactions. The whitecapping parameter (C_{ds}) was detected to be the most effective calibration parameter on model simulations (Yuksel et al., 2020; Islek and Yuksel., 2021; Islek et al., 2021). Therefore, C_{ds} were assigned as a tunable parameter, and to determine the best estimate of wave parameters further calibration and detailed validation tests were performed in the next section.

Results

In this section, the performance of the model using the three different wind fields in the Eastern Mediterranean Sea was assessed and the effects of different resolutions on the model performance were discussed.

The model results were calibrated by comparing wave measurements from the four different stations and were validated by comparing the two different stations along the Eastern Mediterranean Sea coastlines. The characteristics and locations of the six measurement stations are presented in Table 1 and Figure 1, respectively. In this study, among the six measurement stations, Antalya, Dardanelles, and Silifke stations were calibrated and validated according to the peak wave period, and Bozcaada, Dalaman, and Alanya stations were evaluated for their mean wave period records due to the absence of their peak wave period measurements.

Table 1. Characteristics of the measurement stations in the Eastern Mediterranean Sea.

Station Name	Coordinates (°)	Depth (m)	Data Period	Measured Wave Data	Source
Bozcaada	39.704 N 26.049 E	-58	28.11.1994– 26.09.1995	H_s, T_m	Ozhan and Abdalla (2002)
Dalaman	36.692 N 28.755 E	-75	21.11.1994– 29.07.1996	H_s, T_m	Ozhan and Abdalla (2002)
Alanya	36.542 N 31.975 E	-20	01.11.1994– 08.02.1996	H_s, T_m	Ozhan and Abdalla (2002)
Antalya	36.717 N 31.017 E	-330.5	24.03.2015– 20.11.2018	H_s, T_p	Turkish State Meteorological Service (TSMS)
Dardanelles	40.048 N 26.036 E	-48	17.03.2015– 10.11.2018	H_s, T_p	TSMS
Silifke	36.083 N 33.833 E	-277	23.03.2015– 20.11.2018	H_s, T_p	TSMS

Calibration evaluation in the Eastern Mediterranean Sea
To evaluate the model performance, the modeled significant wave height and wave period were compared with wave measurements. The calibration processes were carried out with the measured wave data at Alanya, Bozcaada, Dalaman, and Antalya stations (Figure 1,

Table 1). The calibration process was performed separately for different wind sources to determine the best match between the modeled and measured wave parameters in the Eastern Mediterranean study area. Using ERA-I wind fields, the calibration of the MIKE 21 SW model and details were given by Yuksel et al. (2020). Yuksel et al. (2020) carried out detailed

calibration and validation using ERA-I and the values obtained using C_{ds}=1.5 are very consistent with the whitecapping parameter, with the mean values measured at almost all stations in Table 1.

In this study, considering the optimal model settings given in the *Methods* section detailed calibration for ERA5 and CFSR wind fields was conducted by tuning the whitecapping parameter with values ranging from 1.0 to 3.0. To quantitatively evaluate the calibration of the MIKE 21 SW hindcasts, statistical error results are presented in Table 2 for significant wave heights, and Table 3 for wave periods. The scatter diagrams showing the relationship between the modeled and measured significant wave heights and wave periods at Alanya, Bozcaada, Dalaman, and Antalya stations are shown in Figure 3 and Figure 4, respectively. Quantile-Quantile

(Q-Q) plots to check the accuracy at the lowest/highest percentile can be seen in Figure 5 and Figure 6. PDF (Probability Density Function) plots are investigated given in Figure 7. Detailed time histories comparison between modeled and measured significant wave height and wave period are shown in Figure A.1–Figure A.4.

In the Eastern Mediterranean study area (considering the statistical analysis presented in Table 2 and Table 3) and scatter plots given in Figure 3 and Figure 4, Q-Q plots depicted in Figure 5 and Figure 6, PDF plot given in Figure 7, the modeled wave results (significant wave heights and wave periods) obtained using C_{ds} values ranging from 1.0 to 3.0 show a significant variation for both ERA5 and CFSR winds.

Table 2. Statistical analysis of modeled significant wave height using C_{ds} values ranging from 1.0 to 3.0 against measured significant wave height for the Eastern Mediterranean Sea.

		Measured	C_{ds}=1.0	C_{ds}=1.5	C_{ds}=2.0	C_{ds}=2.5	C_{ds}=3.0
				$H_{s, ERA5}$ (m)			
Alanya	Mean	0.59	0.74	0.66	0.60	0.56	0.53
	Bias		0.14	0.07	0.01	-0.03	-0.06
	RMSE		0.24	0.19	0.17	0.17	0.19
	SI		0.40	0.32	0.29	0.29	0.31
	R		0.91	0.91	0.92	0.92	0.92
Bozcaada	Mean	0.62	0.73	0.67	0.64	0.61	0.58
	Bias		0.11	0.06	0.02	-0.01	-0.03
	RMSE		0.31	0.28	0.26	0.25	0.25
	SI		0.50	0.45	0.42	0.41	0.41
	R		0.84	0.84	0.84	0.84	0.84
Dalaman	Mean	0.55	0.68	0.60	0.56	0.52	0.49
	Bias		0.12	0.05	0.00	-0.04	-0.06
	RMSE		0.23	0.18	0.16	0.16	0.17
	SI		0.41	0.32	0.30	0.30	0.31
	R		0.92	0.92	0.93	0.92	0.92
Antalya	Mean	0.43	0.57	0.51	0.47	0.44	0.41
	Bias		0.14	0.08	0.04	0.01	-0.02
	RMSE		0.24	0.19	0.17	0.16	0.16
	SI		0.56	0.44	0.39	0.37	0.37
	R		0.90	0.90	0.90	0.90	0.90
		Measured	C_{ds}=1.0	C_{ds}=1.5	C_{ds}=2.0	C_{ds}=2.5	C_{ds}=3.0
				$H_{s, CFSR}$ (m)			
Alanya	Mean	0.59	0.76	0.68	0.62	0.58	0.55
	Bias		0.16	0.08	0.03	-0.01	-0.05
	RMSE		0.32	0.24	0.24	0.23	0.23
	SI		0.54	0.45	0.41	0.39	0.39
	R		0.85	0.85	0.85	0.85	0.85
Bozcaada	Mean	0.62	0.77	0.72	0.67	0.64	0.61
	Bias		0.16	0.10	0.06	0.03	-0.01
	RMSE		0.38	0.34	0.31	0.29	0.28
	SI		0.62	0.55	0.50	0.47	0.46
	R		0.82	0.82	0.82	0.82	0.82
Dalaman	Mean	0.55	0.69	0.62	0.57	0.53	0.50
	Bias		0.14	0.06	0.01	-0.03	-0.06
	RMSE		0.31	0.25	0.23	0.21	0.21
	SI		0.56	0.46	0.41	0.39	0.38
	R		0.88	0.89	0.89	0.89	0.89
Antalya	Mean	0.43	0.52	0.46	0.42	0.39	0.36
	Bias		0.09	0.03	-0.01	-0.04	-0.07
	RMSE		0.23	0.20	0.19	0.19	0.20
	SI		0.53	0.45	0.43	0.44	0.45
	R		0.86	0.87	0.87	0.87	0.87

Table 1. Statistical analysis of modeled wave period using C_{ds} values ranging from 1.0 to 3.0 against measured wave period for the Eastern Mediterranean Sea.

		Measured	C_{ds}=1.0	C_{ds}=1.5	C_{ds}=2.0	C_{ds}=2.5	C_{ds}=3.0
					$T_{m, ERA5}$ (s)		
Alanya	Mean	4.22	4.41	4.30	4.22	4.16	4.10
	Bias		0.18	0.08	0.00	-0.07	-0.12
	RMSE		0.60	0.57	0.56	0.57	0.58
	SI		0.14	0.13	0.13	0.13	0.14
	R		0.80	0.80	0.80	0.80	0.80
Bozcaada	Mean	3.01	3.14	3.08	3.04	3.01	2.97
	Bias		0.13	0.07	0.03	-0.01	-0.04
	RMSE		0.46	0.44	0.44	0.44	0.44
	SI		0.15	0.15	0.15	0.14	0.15
	R		0.80	0.80	0.80	0.80	0.79
Dalaman	Mean	3.93	3.78	3.66	3.57	3.50	3.44
	Bias		-0.15	-0.28	-0.37	-0.44	-0.49
	RMSE		0.65	0.70	0.75	0.79	0.83
	SI		0.17	0.18	0.19	0.20	0.21
	R		0.72	0.72	0.71	0.70	0.70
					$T_{p, ERA5}$ (s)		
Antalya	Mean	4.56	4.86	4.69	4.57	4.47	4.40
	Bias		0.30	0.13	0.01	-0.09	-0.17
	RMSE		1.13	1.11	1.12	1.15	1.17
	SI		0.25	0.24	0.25	0.25	0.26
	R		0.59	0.59	0.58	0.56	0.55
		Measured	C_{ds}=1.0	C_{ds}=1.5	C_{ds}=2.0	C_{ds}=2.5	C_{ds}=3.0
					$T_{m, CFSR}$ (s)		
Alanya	Mean	4.22	4.27	4.15	4.05	3.98	3.91
	Bias		0.04	-0.08	-0.17	-0.24	-0.31
	RMSE		0.76	0.76	0.78	0.80	0.82
	SI		0.18	0.18	0.18	0.19	0.19
	R		0.72	0.72	0.72	0.71	0.71
Bozcaada	Mean	3.01	3.18	3.12	3.07	3.04	3.00
	Bias		0.17	0.11	0.06	0.03	-0.01
	RMSE		0.56	0.54	0.53	0.52	0.52
	SI		0.18	0.18	0.17	0.17	0.17
	R		0.76	0.76	0.76	0.76	0.76
Dalaman	Mean	3.93	3.74	3.61	3.51	3.43	3.37
	Bias		-0.19	-0.33	-0.43	-0.50	-0.57
	RMSE		0.75	0.81	0.87	0.92	0.96
	SI		0.19	0.21	0.22	0.23	0.24
	R		0.68	0.67	0.65	0.64	0.63
					$T_{p, CFSR}$ (s)		
Antalya	Mean	4.56	4.93	4.75	4.61	4.50	4.41
	Bias		0.37	0.18	0.05	-0.06	-0.15
	RMSE		1.25	1.21	1.20	1.21	1.23
	SI		0.27	0.27	0.26	0.27	0.27
	R		0.56	0.57	0.57	0.56	0.56

Using ERA5 wind fields, the change of the tunable parameter (whitecapping parameter C_{ds}) by increasing/reducing has a significant effect on the bias. However, the correlation coefficient (R) does not change markedly (0.92±0.01). According to the statistical error results (Table 2 and Table 3), the RMSE and SI index significantly increase when reducing C_{ds} from the value of 2.0. On the other hand, similar increasing statistical error results were observed when increasing C_{ds} from the value of 2.0. The mean values of modeled wave results obtained using C_{ds}=2.0 are very consistent with the mean values measured at almost all stations. CFSR wind fields, as obtained with model results using ERA5 wind fields, show essentially similar effects to those obtained by adjusting the whitecapping parameter (C_{ds}). In general, at all measurement stations, the best model results were obtained with the value of C_{ds}=2.0. It is

noted that the correlation coefficient obtained using CFSR (0.89±0.01) is lower than compared obtained using ERA5. According to the statistical error results determined using CFSR wind fields (Table 2), a slightly lower accuracy in the model results was determined, i.e., the statistical error measures (bias, RMSE, and SI) were calculated higher than those obtained using ERA5. At almost all measured stations, the significant wave height and wave period modeled using CFRS wind fields were slightly overestimated compared to results for ERA5, except for the Antalya station. This difference between the results of the two data sources may be due to both different temporal and spatial resolutions, and different data assimilation techniques (4D-Var using IFS Cycle 41r2 for ERA-5 vs 3D-Var for CFSR) (Islek et al., 2020).
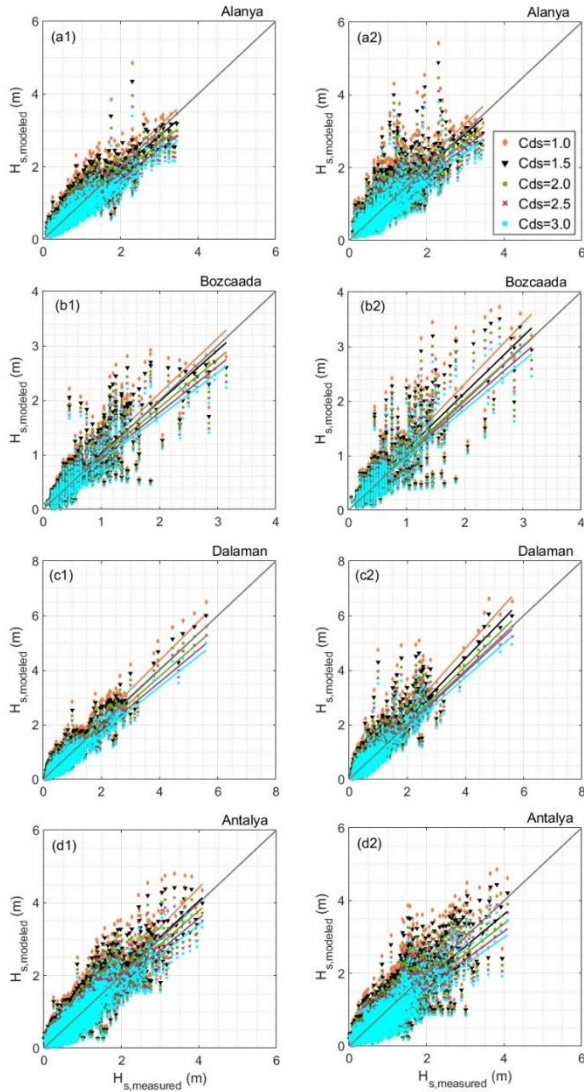
Figure 3. Scatter diagrams of the significant wave height obtained from the model using $C_{ds}=1.0-3.0$ against the measured significant wave height at Alanya, Bozcaada, Dalaman, and Antalya stations. Plots numbered 1, and 2 represent the results for ERA5, and CFSR datasets, respectively.
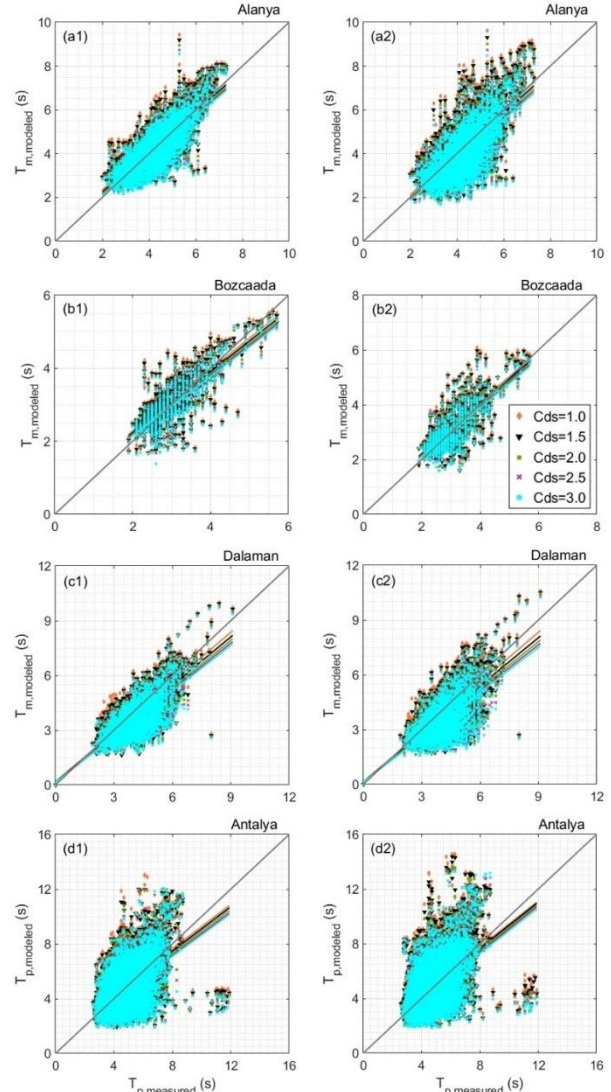
Figure 4. Scatter diagrams of the wave period obtained from the model using $C_{ds}=1.0-3.0$ against the measured wave period at Alanya, Bozcaada, Dalaman, and Antalya stations. Plots numbered 1, and 2 represent the results for ERA5, and CFSR datasets, respectively.

Quantile-Quantile (Q-Q) plot is widely used to evaluate the performance between the modeled and measured data (Aarnes et al., 2017; Christakos et al., 2019; Islek et al., 2022). Q-Q plots show different performances for different classes of the significant wave height and wave period.

At Alanya station, the measured and modeled significant wave height and mean wave period were reasonably well matched up to 2.5 m and 6.0 s, respectively. In higher percentiles, the modeled wave results were more scattered (more prominent when it exceeds 3.4 m for H_s, 6 s for T_m) for both ERA5 and CFSR (Figure 5a1 and b1, Figure 6a1 and b1).

At Bozcaada station, better estimations of the significant wave height and mean wave period were obtained up to 2.2 m and 6.0 s for both ERA5 and CFSR datasets, respectively. The modeled wave results were more

scattered for higher classes of the significant wave height (especially, exceeding 2.3 m) and mean wave period (especially, exceeding 6.0 s) (Figure 5a2 and b2, Figure 6a2 and b2).

At Dalaman station, in almost all wave height classes, the best model results were detected using the value of $C_{ds}=2.0$ for ERA5. The wave results modeled using CFSR for $C_{ds}=2.0$, reasonably well matched up to 2 m, while the relatively better agreement was determined in higher percentiles (especially, exceeding 2.5 m) (Figure 5a3 and b3). The modeled mean wave period obtained using $C_{ds}=2.0$ was shown good performance up to 7s for both datasets. On the other hand, more scattered data were detected for higher mean wave period classes (especially, exceeding 7 s) (Figure 6a3 and b3).

At Antalya station, more satisfactory model results were obtained using the value of $C_{ds}=2.0$ for both ERA5 and

CFSR. The modeled wave results were underestimated for C_{ds}=2.5 and 3.0, while the modeled wave results were overestimated for C_{ds}=1.0 and 1.5 (Figure 5a4 and b4, Figure 6a4 and b4).

In general, relatively better correspondence was determined between the data at four measurement stations and modeled data with the value of C_{ds}=2.0 for both ERA5 and CFSR datasets (Figures 5 and 6).
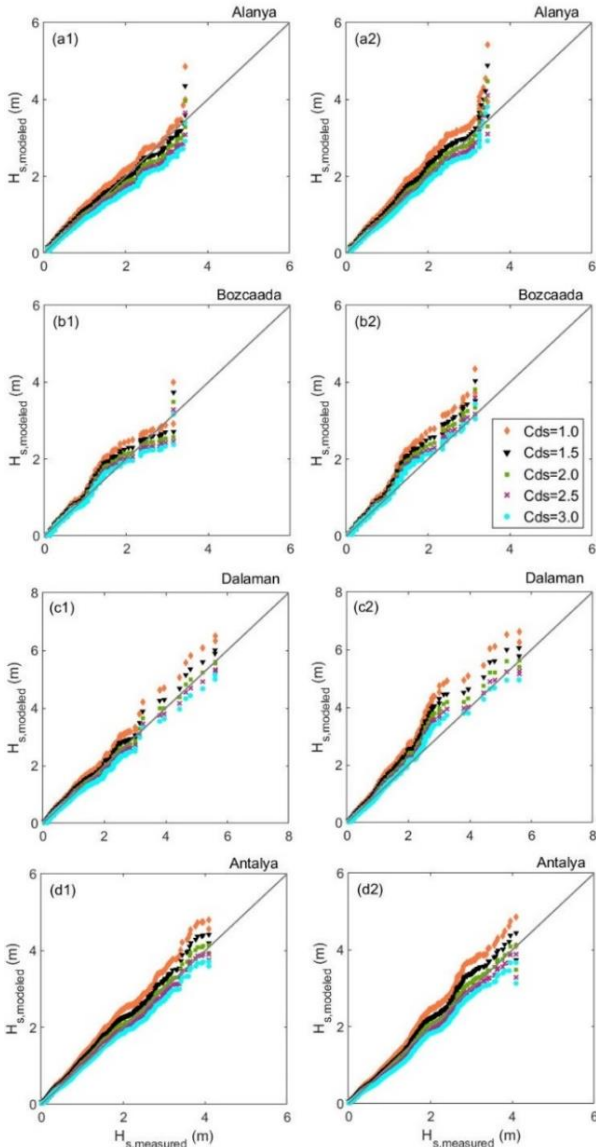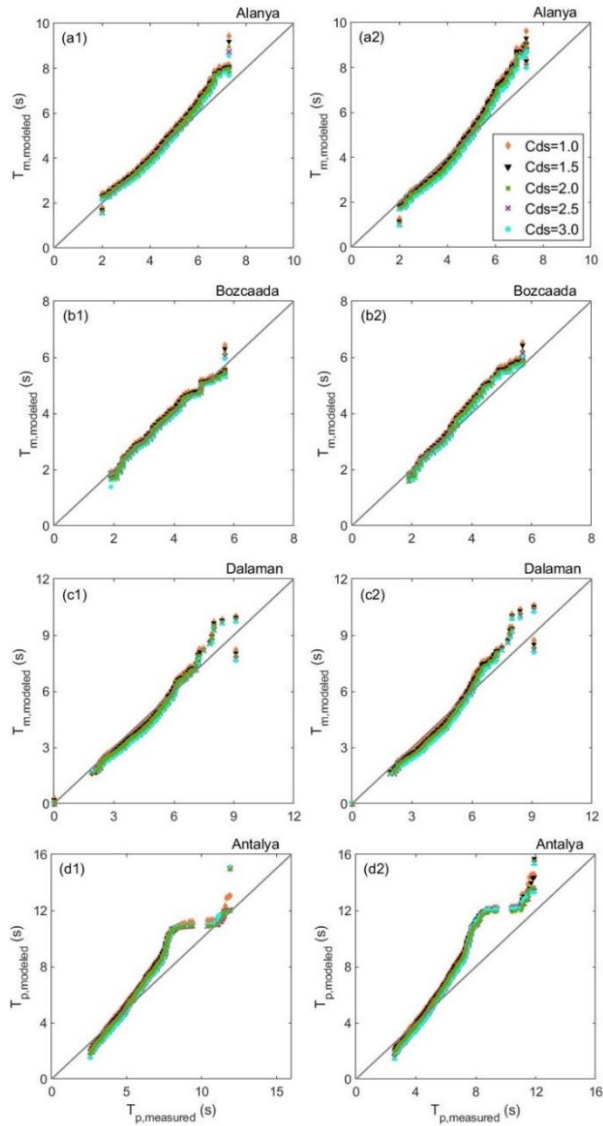

Figure 5. Q-Q plots of significant wave height modeled using three reanalysis wind fields against measured significant wave height at Alanya, Bozcaada, Dalaman, and Antalya, stations. Plots numbered 1, and 2 represent the results for ERA5, and CFSR datasets, respectively

Figure 6. Quantile-Quantile plots of wave period modeled using three reanalysis wind fields against measured wave period at Alanya, Bozcaada, Dalaman, and Antalya stations. Plots numbered 1, and 2 represent the results for ERA5, and CFSR datasets, respectively.

Table 4. Statistics of PDF of H_s at four measurement stations

		Measured	C_{ds}=1.0	C_{ds}=1.5	C_{ds}=2.0	C_{ds}=2.5	C_{ds}=3.0
				$H_{s, ERA5}$ (m)			
Alanya	**Min. (m)**	0.10	0.0972	0.0874	0.0803	0.0728	0.0659
	Mod (m)	0.3	0.4	0.4	0.4	0.3	0.3
	Max. (m)	3.45	4.8551	4.3502	3.9659	3.6563	3.3981
Bozcaada	**Min. (m)**	0.05	0.0294	0.0207	0.0167	0.0148	0.0136
	Mod (m)	0.5	0.5	0.5	0.5	0.5	0.4
	Max. (m)	3.15	2.9213	2.7090	2.5743	2.4694	2.3731
Dalaman	**Min. (m)**	0.05	0.0500	0.0353	0.0250	0.0196	0.0164
	Mod (m)	0.3	0.5	0.4	0.4	0.3	0.3
	Max. (m)	5.60	6.5076	6.0056	5.6088	5.2773	4.9961
Antalya	**Min. (m)**	0.01	0.0612	0.0472	0.0395	0.0345	0.0307
	Mod (m)	0.3	0.4	0.4	0.3	0.3	0.3
	Max. (m)	4.09	4.7994	4.4195	4.1351	3.9037	3.7100

		Measured	C_{ds}=1.0	C_{ds}=1.5	C_{ds}=2.0	C_{ds}=2.5	C_{ds}=3.0
				$H_{s, CFSR}$ (m)			
Alanya	**Min. (m)**	0.10	0.1291	0.1059	0.0884	0.0792	0.0705
	Mod (m)	0.3	0.4	0.4	0.4	0.3	0.3
	Max. (m)	3.45	5.4219	4.8884	4.4667	4.1131	3.8110
Bozcaada	**Min. (m)**	0.05	0.0555	0.0449	0.0397	0.0368	0.0357
	Mod (m)	0.5	0.6	0.5	0.5	0.5	0.5
	Max. (m)	3.15	3.7265	3.5101	3.3298	3.1809	3.0469
Dalaman	**Min. (m)**	0.05	0.0652	0.0483	0.0387	0.0323	0.0277
	Mod (m)	0.3	0.5	0.4	0.4	0.3	0.3
	Max. (m)	5.60	6.6244	6.0590	5.6157	5.2507	4.9457
Antalya	**Min. (m)**	0.01	0.0539	0.0394	0.0320	0.0271	0.0231
	Mod (m)	0.3	0.3	0.3	0.3	0.3	0.3
	Max. (m)	4.09	4.8525	4.4409	4.1316	3.8806	3.6694

Probability Density Function (PDF) of modeled significant wave height obtained using C_{ds}=1.0–3.0 were examined at four measurement stations (Figure 7). The maximum significant wave height was marked in the PDF plots and the main statistical parameters are given in Table 4.

As a result of the increase in the adjustable parameter for whitecapping, the mode and maximum values of H_s gradually decrease for both ERA5 and CFSR datasets. Higher mode values were observed at Bozcaada station, while the greatest maximum significant wave height was detected at Dalaman station for each C_{ds} value. It is important to note that for C_{ds}=2.0, the modeled wave results at Dalaman and Antalya stations have a significantly better fit to the measured significant wave height, and the PDF plots and maximum values exactly overlap. The PDF plot of the significant wave height

modeled with CFSR datasets gave a better fit compared to those obtained with ERA5 datasets (Figure 7a2 and b2). According to wave results for C_{ds}=2.0, reasonably good wave results were determined compared with measurements at Alanya station.

According to C_{ds} values ranging from 0.5 to 3.0, modeled significant wave height for both ERA5 and CFSR datasets is relatively similar. In other words, the two reanalysis datasets were used for determining the Eastern Mediterranean wave properties. One of the most influential key parameters is to determine the optimal tunable calibration parameter, C_{ds}, for reliable wave hindcasts. The PDF plots and their statistical evaluations indicate that the best fit between modeled and measured wave data was detected at all measurement stations when the tunable calibration parameter is C_{ds}=2.0 for both datasets.
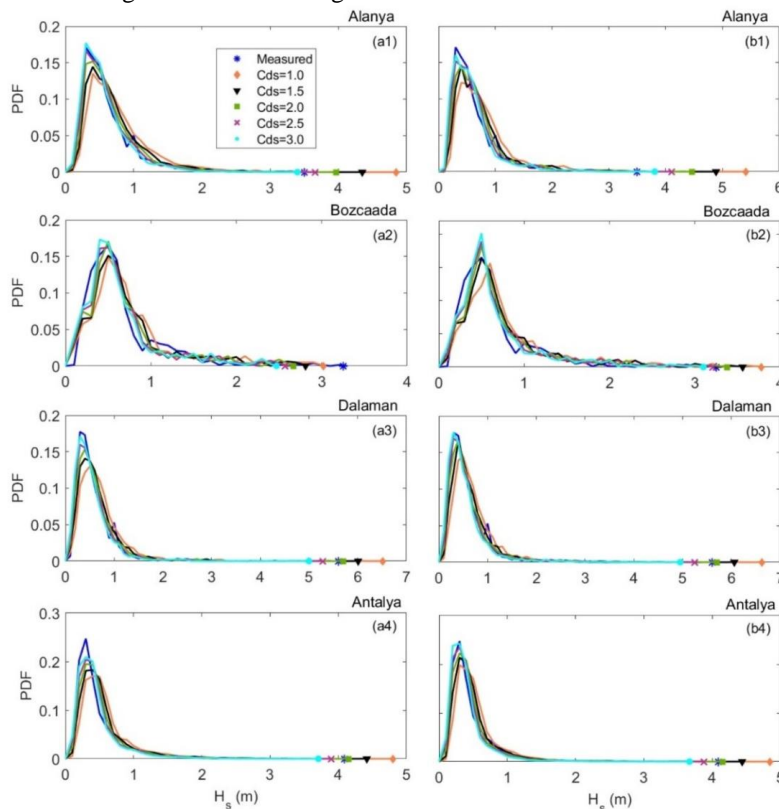

Figure 7. PDF graphics of H_s at four measurement stations. Star, diamond, triangle, square, cross, and circle, represent the maximum significant wave height at Alanya, Bozcaada, Dalaman, and Antalya, respectively. Plots numbered 1, and 2 represent the results for ERA5 and CFSR datasets, respectively

Validation evaluation in the Eastern Mediterranean Sea

The calibrated MIKE 21 SW model was validated at other measurement stations (Dardanelles and Silifke) (Figure 1). The statistical error results are given in Table 5. The scatter diagrams and Q-Q plots at the two stations are depicted in Figure 8 and Figure 9, respectively. For the optimal settings, the comparisons of the time series between the modeled and measured wave parameters are shown in Figure 10. In the validation evaluations, the modeled wave results using ERA-I wind fields were extracted from the dataset produced by Yuksel et al. (2020).

In the Eastern Mediterranean study area, modeled significant wave heights and peak wave periods obtained using ERA-I wind fields were underestimated compared to the wave results obtained with the other two reanalysis wind fields for both Dardanelles and Silifke stations (Figure 8). The differences between wave results modeled with ERA-I and CFSR wind fields are mainly dependent on the wind speed ranges, which are known to have higher wind speed estimates for CFSR than those for ERA-I. Although the modeled wave results using ERA5 and CFSR datasets were in reasonably good agreement with the wave data measured at two stations, considering the statistical error results presented in Table 5, ERA5 gave better accuracy compared to the results based on CFSR. Among the three different wind sources, it is easily identified from Table 5 that the modeled significant wave heights and peak wave periods obtained using ERA5 wind fields have the largest correlation coefficient (R), the lowest bias, RMSE, and SI compared to the results for CFSR and ERA-I.

Table 5. Statistical analysis of modeled significant wave height and peak wave period at Dardanelles and Silifke stations

Q-Q plots indicate that, at Dardanelles station, ERA5 presents a slightly better performance in the prediction of significant wave height and peak wave period compared to wave results obtained with CFSR and ERA-I datasets (Figure 9).

At Silifke station, measured and modeled significant wave height reasonably well matched up to 3.5 m and a relatively better representation was determined for ERA5. On the other hand, significant wave height modeled using three datasets show more scattered in higher percentiles (especially exceeding 3.5 m). In almost all wave period classes, more satisfactory model results were obtained for ERA5 (Figure 9).

The time histories between the modeled and measured significant wave heights and peak wave periods at Silifke station for the years 2015 and 2016 are shown in Figure 10, as an example. In general, the concordance of comparisons for wave results was found to be satisfactorily good for the three different datasets. However, ERA-I showed slightly less agreement compared with ERA5 and CFSR, because it predicted lower significant wave heights and wave periods than ERA5 and CFSR. Additionally, wave results modeled using CFSR were generally overestimated compared to wave results for ERA-I and ERA5. By referring to Figures 8−10, and Table 5, ERA5 were reasonably better matched to the wave measurements at two validation stations and exhibit the lowest RMSE, SI, and the largest correlation coefficient (R) than those obtained with CFSR and ERA-I.

Table 5. Statistical analysis of modeled significant wave height and peak wave period at Dardanelles and Silifke stations

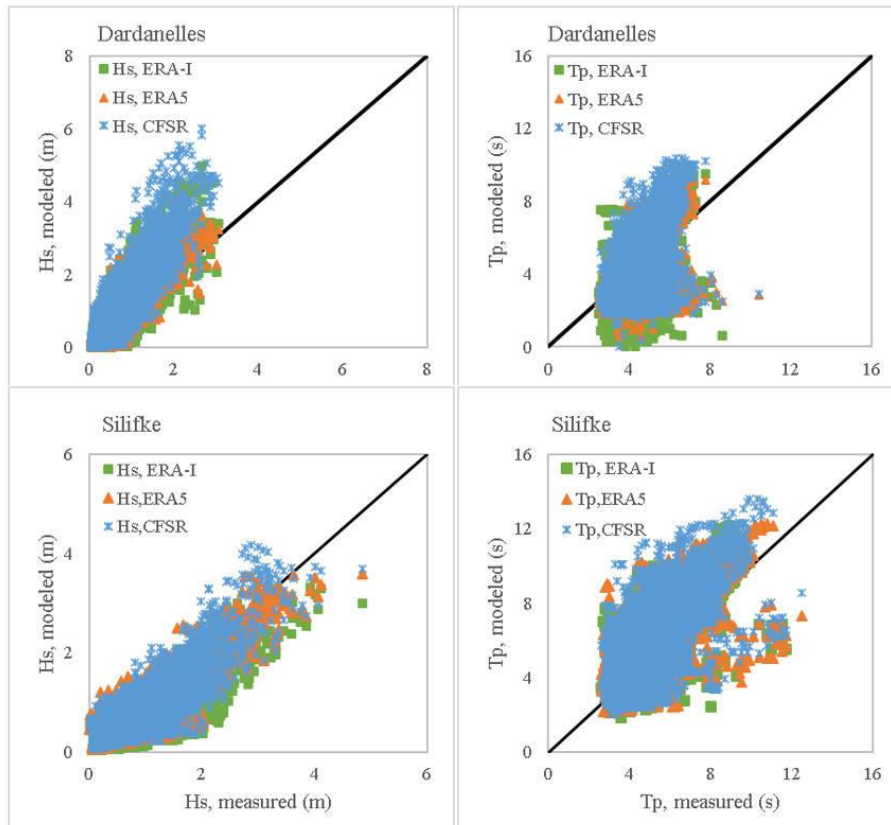|	Mean (m)	Bias (m)	RMSE (m) H_s	SI	R	Mean (s)	Bias (s)	RMSE (s) T_p	SI	R
Dardanelles (2015−2018)										
Measured	0.56					4.24				
ERA-I	0.59	0.11	0.35	0.62	0.89	4.29	-0.32	1.20	0.28	0.53
ERA5	0.74	0.18	0.31	0.56	0.92	4.05	-0.19	1.06	0.25	0.57
CFSR	0.83	0.27	0.49	0.87	0.91	4.22	-0.01	1.19	0.28	0.57
Silifke (2015−2018)										
Measured	0.72					4.92				
ERA-I	0.74	-0.23	0.35	0.49	0.82	4.94	0.32	1.02	0.21	0.70
ERA5	0.66	-0.06	0.21	0.29	0.91	5.29	0.37	0.99	0.20	0.75
CFSR	0.63	-0.09	0.26	0.36	0.85	5.46	0.55	1.27	0.26	0.70

Figure 8. Validation of the calibrated MIKE 21 SW model results against the measurements for significant wave height and wave period at Dardanelles and Silifke stations.
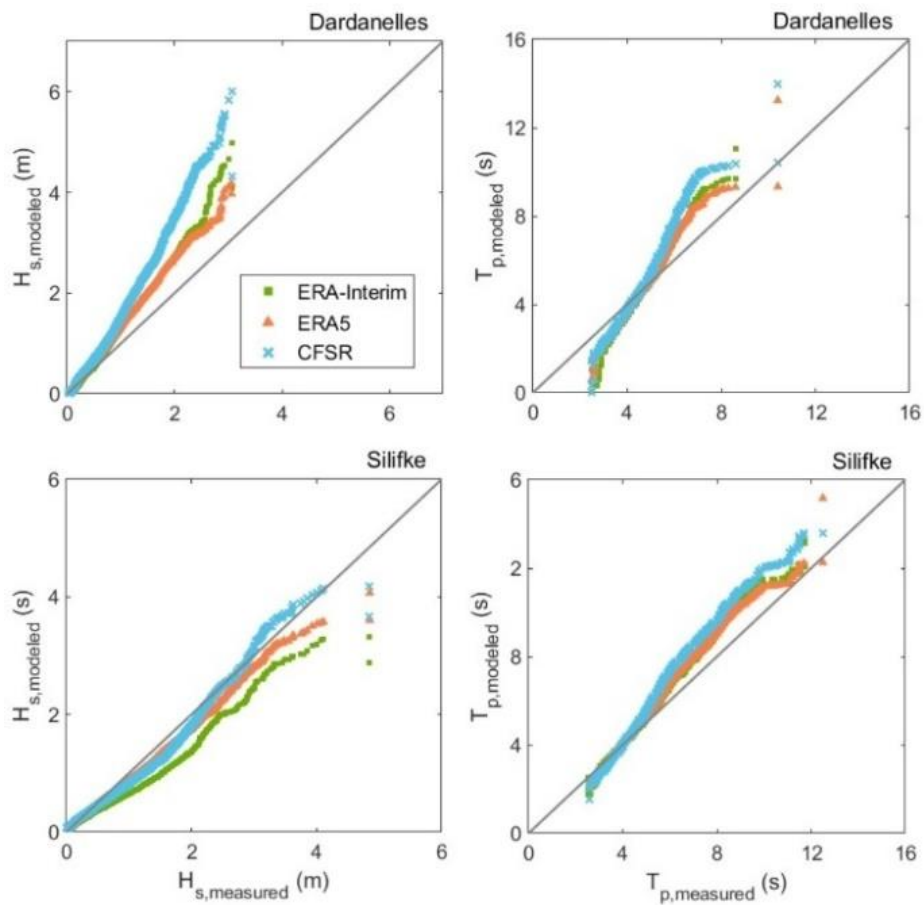

Figure 9. Quantile-Quantile plots of significant wave height and wave period modeled using three reanalysis wind fields against measured wave period at Dardanelles and Silifke stations.
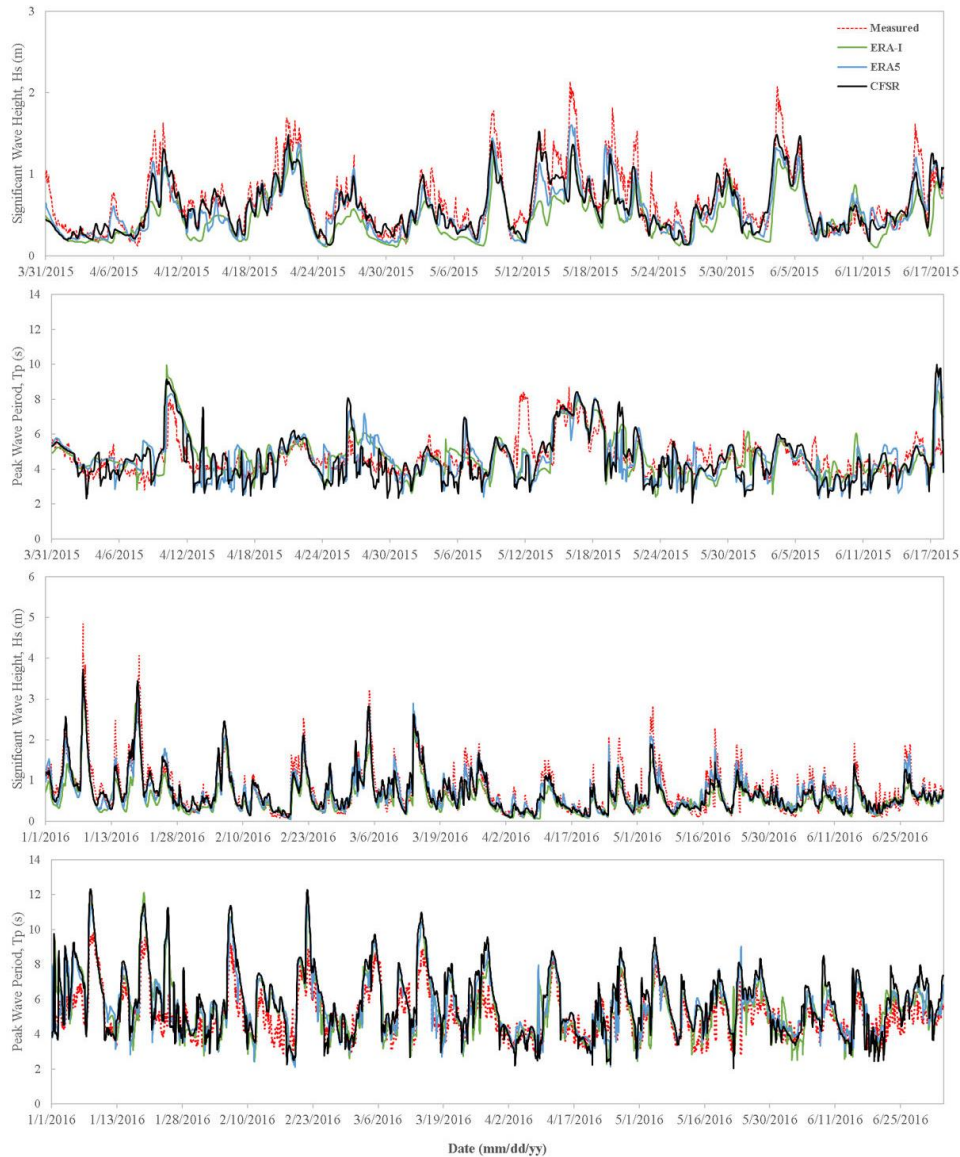
Figure 10. Comparison between modeled and measured significant wave heights and peak wave periods at Silifke station for the years 2015 and 2016.

Wave roses based on the modeled significant wave height

To examine the behavior of significant wave height modeled using ERA5 and CFSR datasets, wave roses were generated in 16 directional and 6 wave height magnitude bands based on the MIKE 21 SW model results. Wave roses at measurement stations (Alanya, Bozcaada, Dalaman, Antalya, Dardanelles, and Slifke) are presented in Figure 11.
The dominant waves come from a similar sector and the range of direction for ERA5 and CFSR. The results are summarized as follows:
➢ Alanya, Antalya, and Silifke, located on the northern coast of the Levantine Basin, are heavily exposed to strong waves coming from SW (southwest).
➢ The dominant wave direction is WSW (west-south-west) and relatively high waves come from S

(south), which is the secondary direction, at Dalaman station.
➢ At Bozcaada and Dardanelles stations, located on the northern coast of the Aegean Sea, the prevailing wave direction is NNE (north-north-east), and the secondary direction is SSW (south-south-west).

Discussion and Conclusion

The present study aims to evaluate the effect of different wind sources on a third-generation spectral wave model performance. To achieve the goal, the two widely used reanalysis wind fields, namely ERA-I and CFSR, and the most up-to-date reanalysis dataset, namely ERA5, were used to generate the wave climate in the Eastern Mediterranean Sea. The required wave parameters were generated from the third-generation spectral wave model, MIKE 21 SW, using the three wind datasets as input data. MIKE 21 SW model was calibrated with the measured wave data at Bozcaada, Dalaman Alanya, and

Antalya stations and validated at Silifke and Dardanelles stations located on the Eastern Mediterranean Sea coastlines.
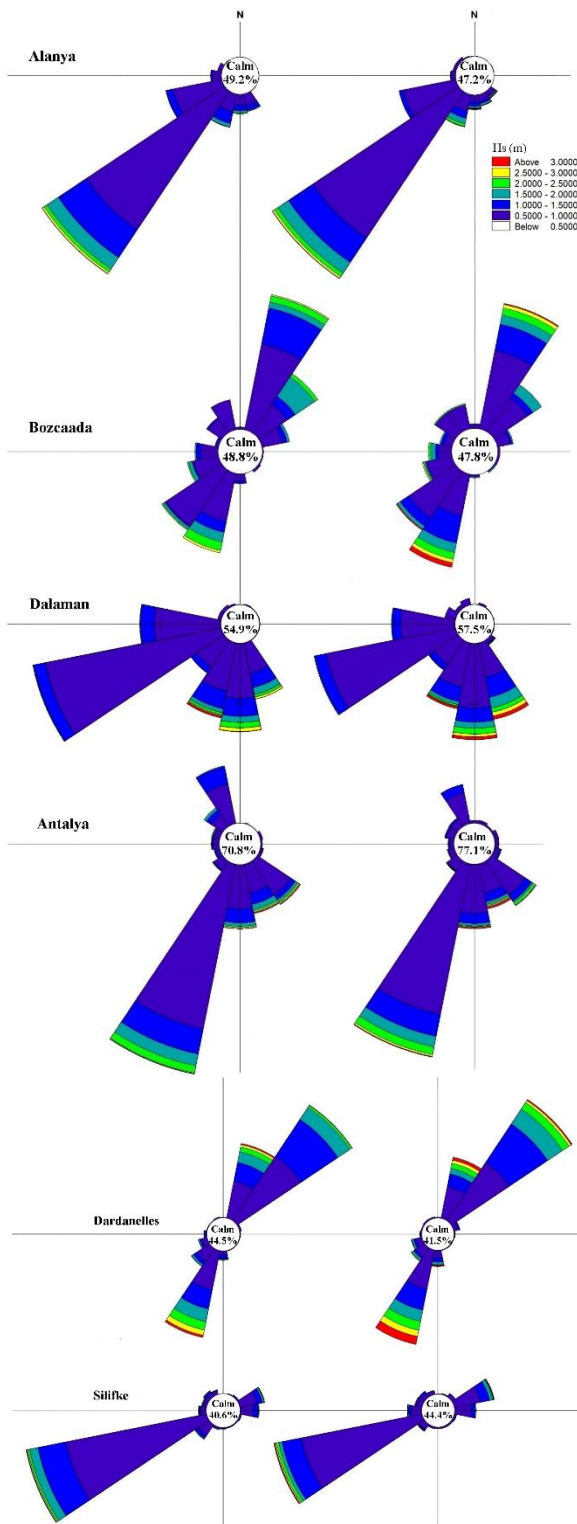

Figure 11. Wave roses at Alanya, Bozcaada, Antalya, Dardanelles, and Silifke stations. The left and right panels show the results obtained from the model using ERA5 and CFSR, respectively.

In the calibration process, to determine the best agreement between the modeled and measured wave parameters, different calibration tests were assessed by changing physical parameters including whitecapping parameter (C_{ds}), bottom friction (k_n), wave breaking (α and γ), and the consideration of triad and/or quadruplet wave interactions. As a result of calibration tests, the adjustable parameter for whitecapping (C_{ds}), which is coupled with the energy transfer from the wind to the waves in the numerical model, was a more effective parameter than the parameters for bottom friction, depth-induced wave-breaking, and nonlinear wave-wave interactions. In the study, the whitecapping parameter (C_{ds}) was used as a tunable calibration parameter.

The calibrated values for physical parameters were determined as follows:

(i) the formulation of Komen et al. (1994) was used for wind input,

(ii) the expression based on the formulation of Komen et al. (1994) was considered for the dissipation due to whitecapping and the values of $C_{ds} = 1.5$ for ERA-I, and $C_{ds} = 2.0$ for both ERA5 and CFSR,

(iii) constant Nikuradese roughness k_n with the value of 0.04 m was utilized for the bottom friction dissipation,

(iv) depth limited wave breaking was considered the formulation based on the bore model by Battjes and Janssen (1978) with α=1 and γ=0.8,

(v) quadruplet wave interaction was computed by using the DIA by Hasselman et al. (1985),

(vi) triad wave interactions were opted out.

Validation of the calibrated MIKE 21 SW model was evaluated by comparing two measurement stations (Dardanelles and Silifke). Overall accuracy was reasonably good for significant wave heights and wave periods. Moreover, the percentages of the calm waves, dominant and secondary wave directions modeled with ERA5 and CFSR are satisfactorily consistent with each other. However, the wave results modeled using ERA-I wind fields showed slightly less agreement than results modeled using ERA5 and CFSR wind fields. The model results obtained using ERA5 wind fields showed the highest correlation coefficient (R), had relatively low statistical error measures (e.g., bias, RMSE), were less scattered data and well-matched with wave measurements, and followed by the wave results obtained using CFSR, and ERA-I. This implies that ERA5 performed slightly better in the prediction of the wave parameters than the other two datasets (ERA-I and CFSR).

References

Aarnes, O.J., Reistad, M., Breivik, Ø., Bitner-Gregersen, E., Ingolf Eide, L., Gramstad, O., Magnusson, A.K., Natvig, B. and Vanem, E. (2017). Projected changes in significant wave height toward the end of the 21st century: Northeast Atlantic. *Journal of Geophysical Research: Oceans, 122(4)*, 3394–3303. https://doi.org/10.1002/2016JC012521

Battjes, J.A. and Janssen, J.P.F.M. (1978). Energy loss and set-up due to breaking of random waves. *Coastal*

Engineering Proceedings, *1*(16), 32. https://doi.org/10.9753/icce.v16.32

Booij, N., Ris, R.C., Holthuijsen, L.H. (1999). A third-generation wave model for coastal regions: 1. Model description and validation. *Journal of Geophysical Research: Oceans, 104 (C4)*, 7649–7666. https://doi.org/10.1029/98JC02622

Cavaleri, L. and Bertotti, L. (2005). The improvement of modeled wind and wave fields with increasing resolution. *Ocean Engineering, 33*, 553–565. https://doi.org/10.1016/j.oceaneng.2005.07.004

Christakos, K., Furevik, B.R., Aarnes, O.J., Breivik, Q., Tuomi, L. and Byrkjedal, Q. (2019). The importance of wind forcing in fjord wave modelling. *Ocean Dynamics, 70*, 57–75. https://doi.org/10.1007/s10236-019-01323-w

Dee, D.P., Uppala, S.M., Simmons, A.J., Berrisford, P., Poli, P., Kobayashi, S., Andrae, U., Balmaseda, M.A., Balsamo, G., Bauer, P., Bechtold, P., Beljaars, A.C.M., van de Berg, L., Bidlot, J., Bormann, N., Delsol, C., Dragani, R., Fuentes, M., Geer, A.J., Haimberger, L., Healy, S.B., Hersbach, H., Holm, E.V., Isaksen, L., Kallberg, P., Kohler, M., Matricardi, M., McNally, A.P., Monge-Sanz, B.M., Morcrette, J.J., Park, B.K., Peubey, C., de Rosnay, P., Tavolato, C., Thepaut, J.N., Vitart, F. (2011). The ERA-interim reanalysis: configuration and performance of the data assimilation system. *Quarterly Journal of the Royal Meteorological Society, 137*, 553–597. https://doi.org/10.1002/qj.828

DHI (2007). MIKE 21-Spectral Wave Module-Scientific Document, 42.

Elkut, A.E., Taha, M.T., Abu Zed, A.E., Eid, F.M., Abdallah, A.M, (2021). Wind-wave hindcast using modified ECMWF ERA-Interim wind field in the Mediterranean Sea. *Estuarine, Coastal and Shelf Science, 252*, 107267. https://doi.org/10.1016/j.ecss.2021.107267

Hasselmann, S., Hasselmann, K., Allender, J.H., Barnett, T. P. (1985). Computations and parameterizations of the nonlinear energy transfer in a gravity-wave spectrum. Part II: Parameterizations of the nonlinear energy transfer for application in wave models. *Journal of Physical Oceanography, 15*, 1378–1391.

Hersbach, H. and Dee, D. (2016). ERA5 reanalysis is in production. *ECMWF Newsletter vol. 147*, 7.

Holthuijsen, L.H., Booij, N., Herbers, T.H.C. (1989). A prediction model for stationary, short-crested waves in shallow water with ambient currents. *Coastal Engineering, 13(1)*, 23–54. https://doi.org/10.1016/0378-3839(89)90031-8

Islek, F., Yuksel, Y., Sahin, C. (2020). Spatiotemporal long-term trends of extreme wind characteristics over the Black Sea. *Dyn. Atmos. Ocean. 90*, 101132. https://doi.org/10.1016/j.dynatmoce.2020.101132

Islek, F., Yuksel, Y., Sahin, C., Ari Guner, H.A. (2021). Long-term analysis of extreme wave characteristics based on the SWAN hindcasts over the Black Sea. *Dynamics of Atmospheres and Oceans, 94*, 101165. https://doi.org/10.1016/j.dynatmoce.2020.101165

Islek, F. and Yuksel, Y. (2021). Inter-comparison of long-term wave power potential in the Black Sea based on the SWAN wave model forced with two

different wind fields. *Dynamics of Atmospheres and Oceans, 93*, 101192. https://doi.org/10.1016/j.dynatmoce.2020.101192

Islek, F., Yuksel, Y., Sahin C. (2022). Evaluation of regional climate models and future wind characteristics in the Black Sea. *International Journal of Climatology, 42(3)*, 1877–1901. https://doi.org/10.1002/joc.7341

Komen, G.J., Cavaleri, L., Donelan, M., Hasselmann, K., Hasselmann, S., Janssen P.A.E.M. (1994). *Dynamics and Modelling of Ocean Waves, Cambridge University Press, UK.*

Mentaschi, L., Besio, G., Cassola, F., Mazzino, A. (2015). Performance evaluation of Wavewatch III in the Mediterranean Sea. *Ocean Modelling, 90*, 82–94. https://doi.org/10.1016/j.ocemod.2015.04.003

Music, S., and Nikovic, S. (2008). 44-year wave hindcast for the Eastern Mediterranean. *Coastal Engineering, 55(11)*, 872-880. https://doi.org/10.1016/j.coastaleng.2008.02.024

Ozhan, E., and Abdalla, S. (2002). Wind and Deep Water Wave Atlas of Turkish Coasts, Turkish National Coastal Zone Management Committee/MEDCOAST. *Middle East Technical University, Ankara,* pp. 445.

Ponce de León, S. and Guedes Soares, C. (2008). Sensitivity of wave model predictions to wind fields in the Western Mediterranean Sea, *Coastal Engineering, 55(11)*, 920–929, https://doi.org/10.1016/j.coastaleng.2008.02.023

Saha, S., Moorthi, S., Pan, H.-L., Wu, X., Wang, J., Nadigai, S., Tripp, P., Kistler, R., Woollen, J., Behringer, D., Liu, H., Stokes, D., Grumbine, R., Gayno, G., Wang, J., Hou, Y.-T., Chuang, H.-Y., Juang, H.-M.H., Sela, J., Iredell, M., Treadon, R., Kleist, D., van Delst, P., Keyser, D., Derber, J., Ek, M., Meng, J., Wei, H., Yang, R., Lord, S., van den Dool, H., Kumar, A., Wang, W., Long, C., Chelliah, M., Xue, Y., Huang, B., Schemm, J.-K., Ebisuzaki, W., Lin, R., Xie, P., Chen, M., Zhou, S., Higgins, W., Zou, C.-Z., Liu, Q., Chen, Y., Han, Y., Cucurull, L., Reynolds, R.W., Rutledge, G., Goldberg, G. (2010). The NCEP climate forecast system reanalysis. *Bulletin of the American Meteorological Society, 91(8)*, 1015–1057. https://doi.org/10.1175/2010BAMS3001.1

Saha, S., Moorthi, S., Wu, X., Wang, J., Nadiga, S., Tripp, P., Behringer, D., Hou, Y.-T., Chuang, H., Iredell, M., Ek, M., Meng, J., Yang, R., Mendez, M.P., van den Dool, H., Zhang, Q., Wang, W., Chen, M., Becker, E. (2014). The NCEP climate forecast system version 2. *Journal of Climate, 27(6)*, 2185–2208. https://doi.org/10.1175/JCLI-D-12-00823.1

Swain, J. (1997). Simulation of Wave Climate for the Arabian Sea and Bay of Bengal, *PhD Thesis. Naval Physical and Oceanographic Laboratory, Kochi.*

Tolman, H.L. (1991). A third-generation model for wind waves on slowly varying, unsteady, and inhomogeneous depths and currents. *Journal of Physical Oceanography, 21(6)*, 782–797. https://doi.org/10.1175/1520-0485(1991)021<0782:ATGMFW>2.0.CO;2

WAMDI Group (1988). The WAM model – a third generation ocean wave prediction model. *Journal of Physical Oceanography, 18(12)*, 1775–1810. https://doi.org/10.1175/1520-0485(1988)018<1775:TWMTGO>2.0.CO;2

Vannucchi, V., Taddei, S., Capecchi, V., Bendoni m., Brandini, C. (2021). Dynamical Downscaling of ERA5 data on the North-Western Mediterranean Sea: from atmosphere to high-resolution coastal wave climate. *Journal of Marine Science Engineering, 9(2)*, 208. https://doi.org/10.3390/jmse9020208

Yuksel, Y., Yuksel, Z.T., Sahin C. (2020). Effect of long-term wave climate variability on performance-based design of coastal structures. *Aquatic Ecosystem Health & Management, 23(4)*, 407-416, https://doi.org/10.1080/14634988.2020.1807302

Appendix

Fig. A.1. Comparison between significant wave heights modeled using ERA5 wind fields and measured at Alanya, Bozcaada, Dalaman, and Antalya stations.
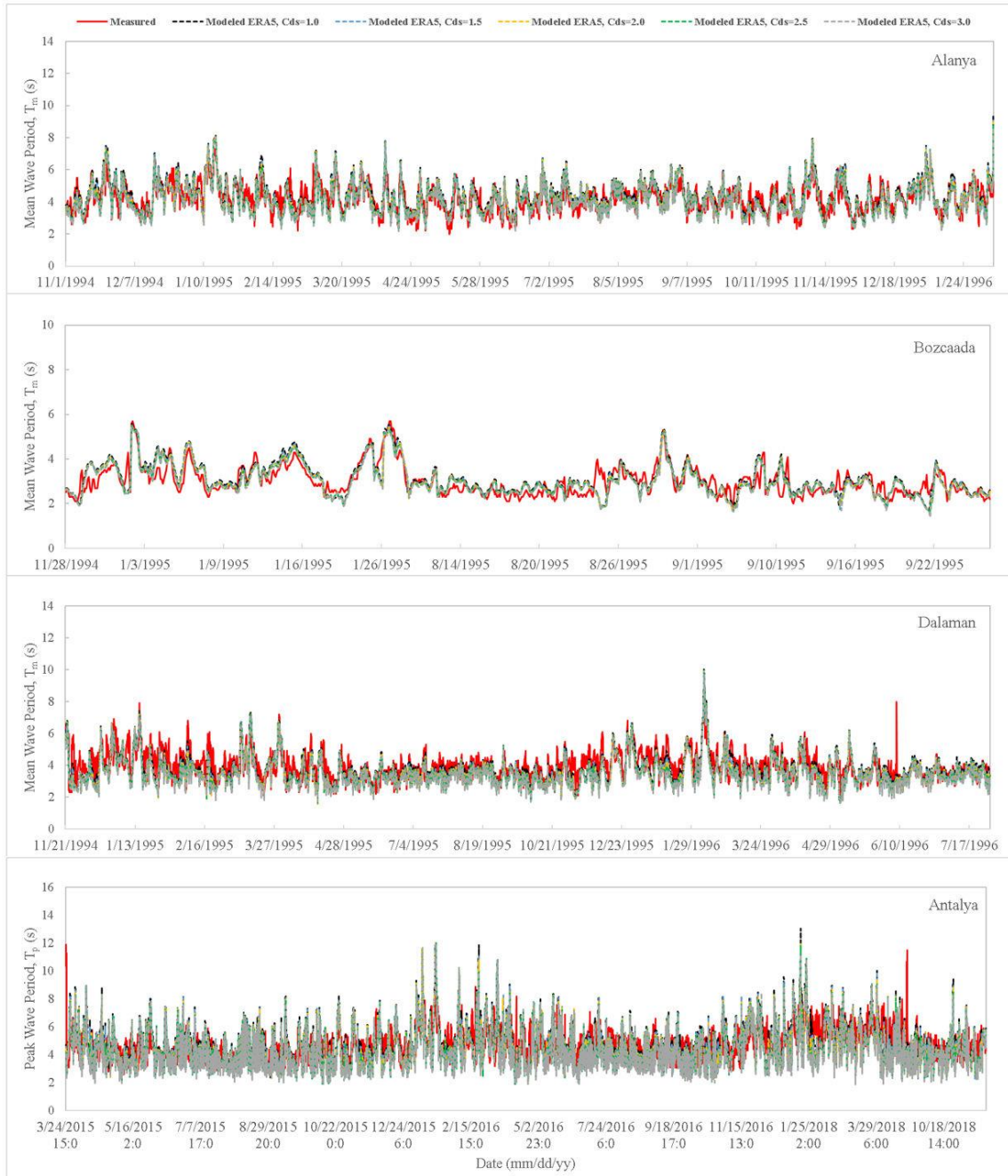
Fig. A.2. Comparison between wave periods modeled using ERA5 wind fields and measured at Alanya, Bozcaada, Dalaman, and Antalya stations.
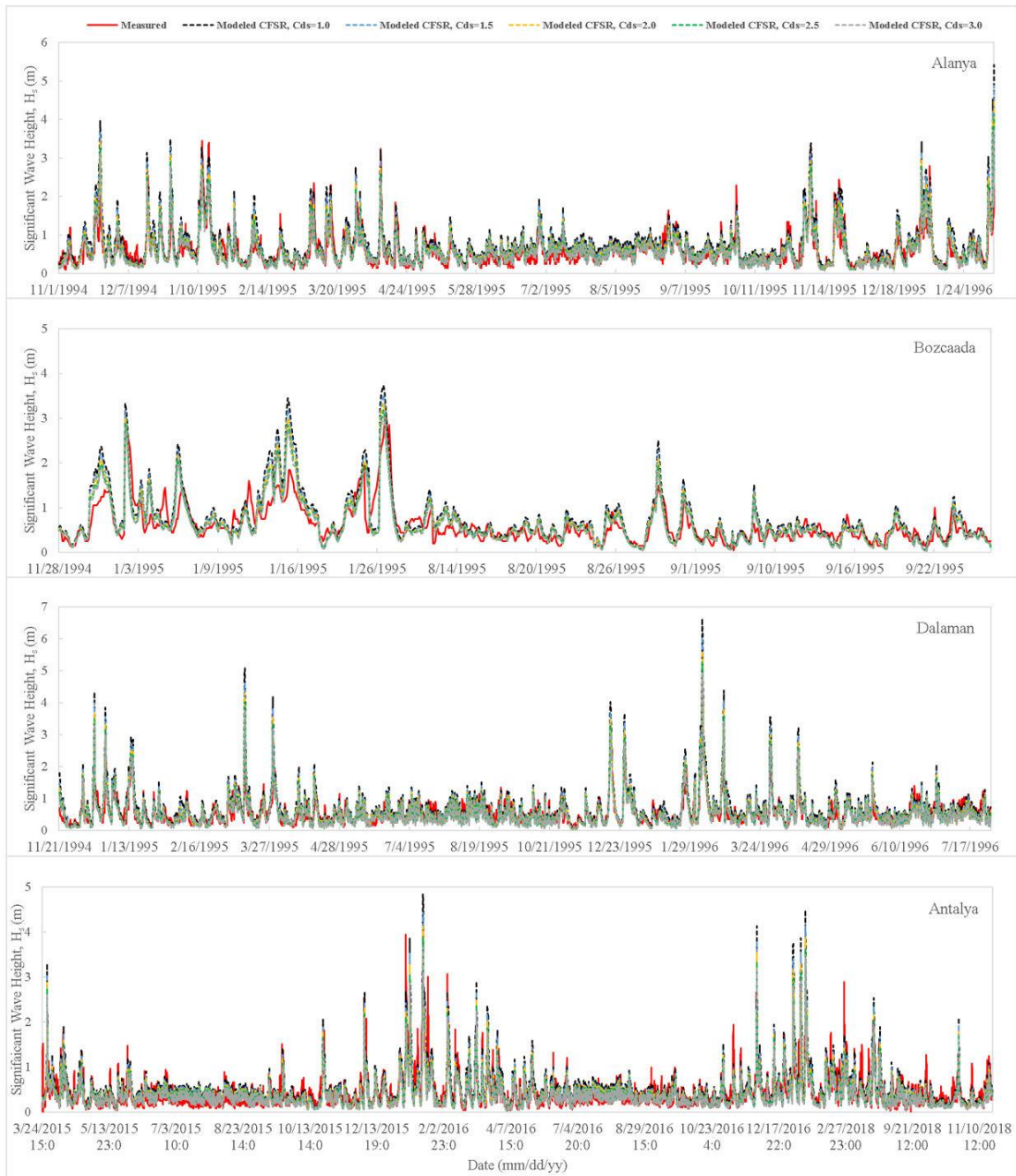
Fig. A.3. Comparison between significant wave heights modeled using CFSR wind fields and measured at Alanya, Bozcaada, Dalaman, and Antalya stations.
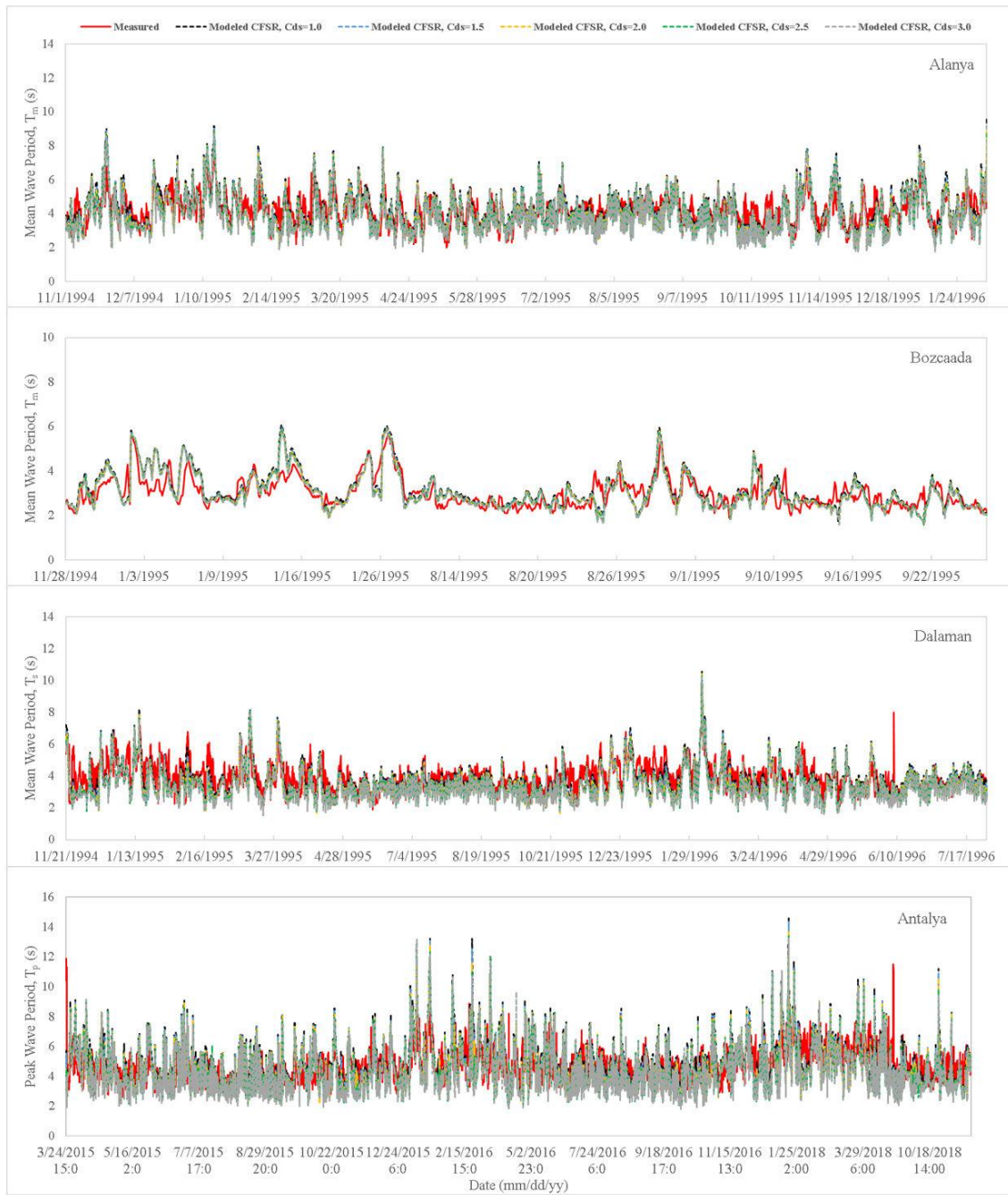
Fig.. A.4. Comparison between wave periods modeled using CFSR wind fields and measured at Alanya, Bozcaada, Dalaman, and Antalya stations.